Nanotechnology to Improve Detection Sensitivity for Electrochemical Microdevices

Masatoshi Yokokawa, Daisuke Itoh, and Hiroaki Suzuki

Abstract With the increase in demands and applications, techniques to create electrochemical microdevices have made a remarkable progress over the last four decades. Key components of the electrochemical devices are electrodes that are easily fabricated by microfabrication techniques. Because of this, miniaturization, batch-fabrication, and integration with other components can easily be realized. This is a contrast to devices based on other detection principles. Miniaturization of the devices also brings with it additional advantages such as very small consumption of sample and reagent solutions, rapid mixing, and parallel processing. On the other hand, however, a challenging issue we often encounter is that it becomes increasingly difficult to maintain the performance that has been achieved by conventional electrochemical devices used in laboratories. To cope with the problem, nanotechnology provides good solutions. Numerous papers have been published to demonstrate the effectiveness of nanotechnology. Therefore, it is impossible to cover all the contents. However, a convincing conclusion is that nanotechnology really has surprising effects on sensing performance. With the wealth of knowledge of nanotechnology, their application to microfabricated devices will be the subject of the next stage. In this chapter, nanotechnologies applicable to the improvement of the performance of existing microfabricated electrochemical devices will be introduced. Although various techniques have been developed for single independent electrodes, those that may be difficult to apply to microfabricated devices are excluded. On the other hand, those that are applicable to nanoelectrodes are included.

Keywords Electrochemical detection, Nanoelectrode, Array, Ensemble, Electrochemiluminescence, Nanofabrication

M. Yokokawa, D. Itoh and H. Suzuki (✉)
Graduate School of Pure and Applied Sciences, University of Tsukuba, 1-1-1 Tennodai, Tsukuba, Ibaraki 305-8573, Japan
e-mail: hsuzuki@ims.tsukuba.ac.jp

A. Tuantranont (ed.), *Applications of Nanomaterials in Sensors and Diagnostics*, Springer Series on Chemical Sensors and Biosensors (2013) 14: 257–280
DOI 10.1007/5346_2012_39, © Springer-Verlag Berlin Heidelberg 2012,
Published online: 8 December 2012

Contents

1 Microelectrodes and Nanoelectrodes 258
1.1 Properties of Independent Micro-/Nano-electrodes 258
1.2 Redox Cycling 260
2 Activation of Electrodes Using Nanostructures 263
2.1 Activation of Electrode Reactions 263
2.2 Promotion of Direct Electron Transfer 265
2.3 Activation of Electrochemiluminescence 265
3 Fabrication of Nanoelectrode Arrays and Ensembles 269
3.1 Formation of Nanoelectrode Arrays by Electron-Beam Lithography or Focused Ion Beam Milling 270
3.2 Formation of Nanoelectrode Arrays by Photolithography 271
3.3 Formation of a Layer of Randomly Oriented CNTs 273
3.4 Formation of CNT Nanoelectrode Ensembles 273
3.5 Formation of Nanoelectrode Ensembles Using a Template 273
3.6 Other Techniques 274
4 Concluding Remarks 275
References 275

1 Microelectrodes and Nanoelectrodes

1.1 Properties of Independent Micro-/Nano-electrodes

To realize highly sensitive detection in a solution of a very small volume, microelectrodes are effective [1, 2]. Typical dimensions of reported microelectrodes are from tens of μm down to sub-μm. Actually, however, there is no clear-cut boundary, and a microelectrode should refer to an electrode whose characteristic dimension is comparable with or smaller than the diffusion layer thickness [3]. The thickness varies as time elapses, which also affects electrode behavior. Here, let us suppose that a sufficiently large overpotential is applied to a microdisk electrode to oxidize or reduce a compound. The diffusion of the molecules to the electrode is quite different from that observed with electrodes usually used in laboratories. With a planar electrode of the mm order for example, the analyte molecules are depleted at the electrode surface and diffuses uniformly from the bulk of the solution to the electrode surface except for the edges of the electrode. On the other hand, with the microelectrode, analyte molecules move towards the electrode along the concentration gradient in the diffusion layer (Fig. 1).

The enhanced diffusion brings with it some advantages. These include a current increase, increase in the signal-to-noise ratio, fast establishment of the steady-state signal, and reduction of the influence of solution resistance [3]. As the size of the electrode decreases, the double-layer capacitance also decreases. This results in the reduction of charging current, which is beneficial in conducting a voltammetric analysis by scanning electrode potential.

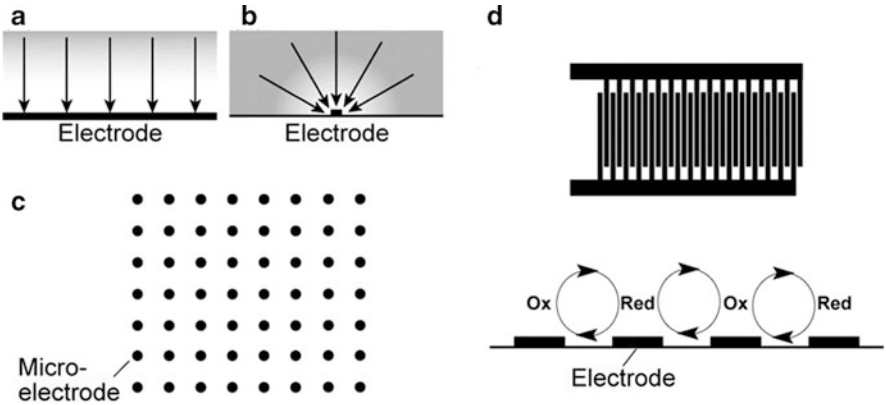

Fig. 1 Diffusion of analyte molecules to a planar electrode of the mm order (**a**) and to a microelectrode (**b**). (**c**) Microelectrode array. (**d**) Interdigitated microelectrodes and redox cycling

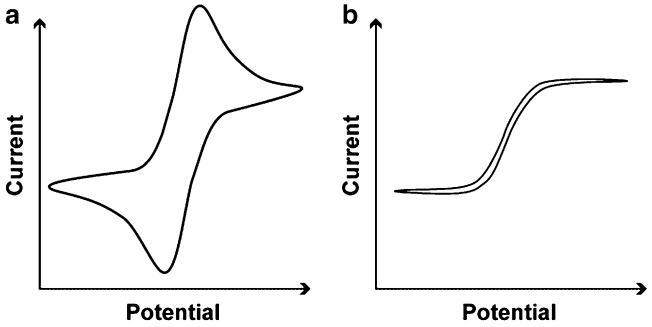

Fig. 2 Cyclic voltammograms observed with an electrode of the mm order (**a**) and with a microelectrode (**b**)

In cyclic voltammograms observed with an electrode of the mm order, for example, redox peaks are observed at scan rates usually used in electrochemical analyses (Fig. 2a). The peaks appear because the rate of mass transport is smaller than that of electrolysis at higher overpotentials, and the molecules that are subject to the electrode reaction continue to decrease in the vicinity of the electrode. On the other hand, with a microelectrode, a sigmoidal curve is observed under a typical condition (Fig. 2b). It should be noted that the shape of the voltammogram also depends on the scan rate of potential. With a very large scan rate, even the microelectrodes show peak-shaped voltammograms. On the other hand, at a very low scan rate, or in a long time scale, even larger electrodes show sigmoidal curves [1].

As mentioned, the microelectrodes have fascinating and excellent properties. However, a problem is its very small current. To solve this problem, microelectrode arrays have been used. In the following discussions, a group of electrodes with controlled shape, dimensions, and an ordered spacing is called an array, whereas a group of electrodes with a random spacing will be called an ensemble. Some geometrical variations are found for the arrays. One is an array of circular electrodes. The other is a row of thin strips of electrodes. The diffusion profile of a microelectrode array shown in Fig. 1c is influenced by the relative interelectrode spacing d/r, where d is the center to center distance and r is the radius of the electrode. With large d/r, the diffusion of the electroactive species to each electrode remains independent of all others. In this case, the limiting current is expressed as the sum of current generated on all the electrodes in the array. On the other hand, with the decrease in d/r, the diffusion layers overlap, and the diffusion profile approaches that of a uniform diffusion observed with a macroscopic electrode with the same geometric area. Although the diffusion is apparently the same as a macroscopic planar electrode, it should be noted that there is a significant difference between the microelectrode array and a macroscopic planar electrode. Because the background and capacitive currents change in proportional to the active area, they are reduced significantly with the microelectrodes. Consequently, substantial improvement in signal-to-noise (SN) ratio and Faradaic-to-capacitive current ratios is achieved with the microelectrode array.

1.2 Redox Cycling

Although the micro/nanoelectrodes themselves are very effective to improve the detection performance, a more fascinating feature called redox cycling can be realized by using two groups of microelectrodes [4]. An orthodox configuration is an interdigitated electrode array (IDA) that consists of a pair of fingers called a generator and a collector. They are held at appropriate different potentials (Fig. 1d). An electroactive analyte undergoes oxidation or reduction on the generator then diffuses to the collector where the analyte undergoes a reverse reaction. The species then diffuses back to the generator, and the cycle is repeated. This results in significant amplification of signal.

The array of micro/nanoelectrodes is not necessarily planar. Figure 3 shows a circular microcavity containing an addressable recessed microdisk gold electrode formed at the bottom and a tubular nanoband gold electrode on the vertical microcavity wall [5]. The microcavity consisted of layers (Fig. 3) consisting of gold layers with a chromium adhesion layer and polyimide insulating layers. The electrodes were separated from each other by 4 μm. The electrode structure was used to cause redox cycling. With this method, electrodes and spacing of the nm order can easily be realized. On the other hand, increasing the number of electrodes will be a tough work.

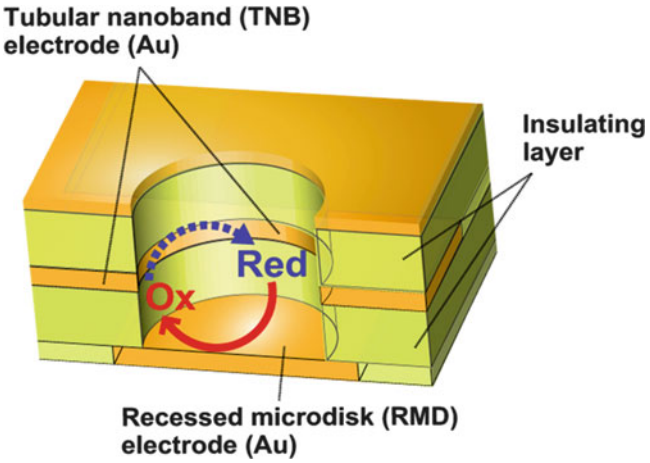

Fig. 3 Redox cycling in a microcavity with a recessed microdisk electrode and tubular nanoband electrodes

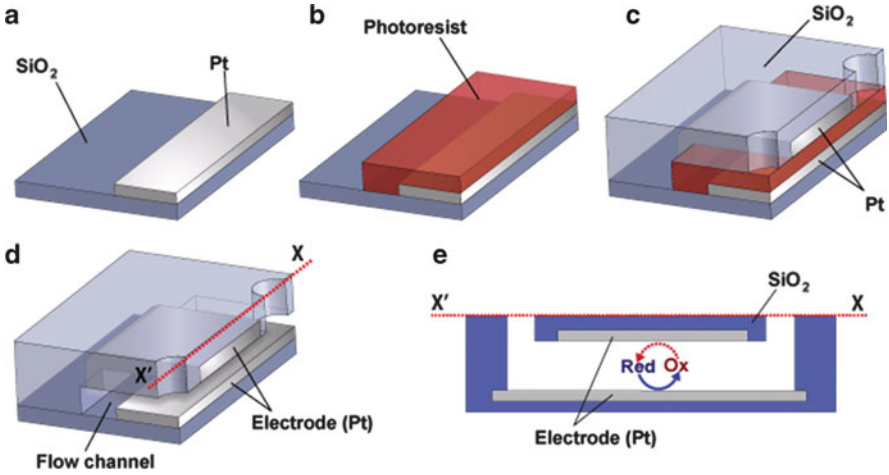

Fig. 4 Fabrication of a nanocavity with a pair of electrodes located at the bottom and ceiling (**a**–**d**). (**e**) Redox cycling caused between the electrodes

Another approach that has a potential to achieve significantly higher amplification is to use a nanocavity [6–9]. A pair of electrodes is located at the bottom and ceiling of a cavity with a height of the nm order. In this device, the electrodes can be simple planar electrodes. Redox cycling occurs between the electrodes facing each other in the nanocavity (Fig. 4).

Although the device uses a nanocavity, the method of formation of the structures is based on the conventional photolithography and micromachining [6–9]. First, the bottom electrode is formed on a substrate (Fig. 4a). Then, a pattern of a sacrificial

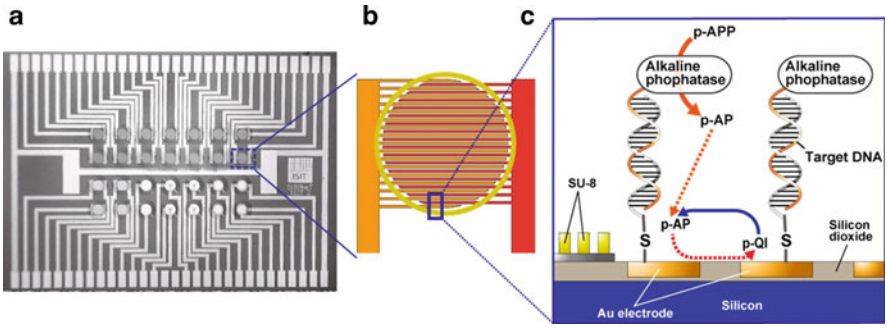

Fig. 5 Chip with multiple detection sites. (**a**) Top view of the chip. (**b**) Magnified view of an IDA electrodes. (**c**) Detection of a target DNA. The DNA binds to a probe DNA linked to the IDA electrodes. Then, the target DNA is enzyme-labeled. A reaction product of the enzymatic reaction p-aminophenole (p-AP) is detected by redox cycling. With kind permission from Springer Science +Business Media: [14]

layer such as photoresist, chromium, or amorphous silicon is formed on the electrode pattern (Fig. 4b). After the top electrode is formed on the sacrificial layer, an insulator layer is formed on the entire structure. Through-holes are formed in the insulating layer to remove the sacrificial layer and to inject a solution to be analyzed (Fig. 4c). Finally, by etching the sacrificial layer away by immersing the structure in an appropriate etchant, the electrode structure separated by a distance of the nm order is formed (Fig. 4d, e). When in use, the nanocavity is filled with an analyte solution and appropriate potentials are applied to the electrodes. Because of the short distance between the electrodes, nearly 100% of the generated product is cycled between the electrodes. With this approach, redox cycling was significantly enhanced, which realized the detection of a few hundred molecules [7].

Redox cycling not only brings with it the amplification of current but also brings additional advantages. In amperometric detection, the interference by electroactive compounds such as L-ascorbic acid, uric acid, and dissolved oxygen poses a problem. However, when the reaction for the analyte is reversible and that for the interferent is irreversible, redox cycling occurs only for the analyte, which suppresses the influence of the interferent relatively.

Redox cycling caused on IDAs has been used for the detection of proteins and DNAs. To couple the molecular recognition of probe molecules to electrochemical detection, the probe molecules are modified with an appropriate enzyme that produces electroactive molecules. One of such enzymes is alkaline phosphatase. This enzyme converts p-aminophenyl phosphate (PAPP) into electroactive p-aminophenol (PAP). PAP is oxidized into quinoneimine, which is also electroactive. In some reported cases, IDAs of the sub-μm order have been used to cause redox cycling for this purpose. The technique has been used for the detection of bacteriophages [10, 11], DNA [12], and RNA [12, 13]. An advantage of electrochemical devices is the integration of components. In some of the above-mentioned cases, simultaneous detection of different target molecules on an array of detection sites has been demonstrated (Fig. 5a) [14].

2 Activation of Electrodes Using Nanostructures

2.1 Activation of Electrode Reactions

Faradaic currents that originate from kinetically controlled electrochemical reactions depend on the real surface area of the working electrode rather than the geometric area. Therefore, by increasing the surface area by some orders of magnitude, the Faradaic current of a sluggish reaction can be enhanced. To this end, nanotechnology offers an excellent solution.

Hydrogen peroxide is often detected in biosensors that use enzymes categorized as oxidases. For biosensing, improvement of sensitivity is often required. To activate the surface of a platinum electrode and improve detection sensitivity, a relatively easy and effective method is to use platinum black. The platinum black is formed by electrodepositing platinum from a solution containing chloroplatinic acid. The platinum black has been used for the hydrogen electrode used for the reference electrode. Without the platinum black, the reversible potential of the hydrogen electrode is not expected. For H_2O_2, a significant improvement in the sensitivity has been observed [15]. Another effective structure is mesoporous platinum [16]. The structure is formed by depositing platinum using the three-dimensional structure of lyotropic liquid crystal phases. Voltammograms obtained with an ordinary planar platinum electrode do not exhibit well-defined plateaus for the oxidation and reduction of H_2O_2, which suggests that the response is under mixed kinetic and diffusion control [16]. Furthermore, linearity of the calibration plot is poor with the ordinary platinum electrode particularly at higher concentrations. This problem has also been solved with the mesoporous platinum and the lower detection limit has also been reduced compared with the conventional platinum electrode.

Glucose is one of the critical target analytes for biosensors. Although numerous papers have been published with regard to enzymatic biosensors, an inherent problem in biosensors in general is long-term stability. To solve this problem, non-enzymatic glucose sensors with nanostructures have been proposed. As demonstrated for the detection of hydrogen peroxide, porous structure of platinum is also effective to enhance direct oxidation of glucose [17]. Ordered porous platinum structure can be formed by depositing platinum through cdse-cds crystalline template (Fig. 6a–c) and dissolving the template in hydrofluoric acid (Fig. 6d). A significant increase in Faradaic current originating from the oxidation of glucose has been observed. The response of the electrode showed unique pH dependence with a maximum around pH 9.

Nanostructures can be formed in a variety of other methods. Ordered array of cylindrical platinum mesopores can be obtained by electrodepositing platinum within the aqueous domains of the liquid crystalline phases of oligoethylene oxide nonionic surfactants and removing the surfactant by rinsing with a large volume of deionized water [18]. Highly ordered platinum nanotube arrays have also been used for the direct oxidation of glucose [19]. The platinum nanotube arrays

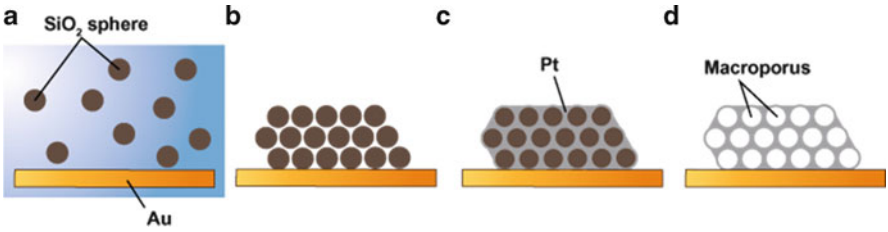

Fig. 6 Fabrication of the platinum microporous structure. (**a–b**) Deposition of SiO_2 spheres on a gold surface. (**c**) Electrodeposition of platinum into the interspace of the SiO_2 template. (**d**) Microporous platinum structure obtained after removing SiO_2 spheres by wet etching

were fabricated by electrodeposition of platinum in the pores of porous anodic alumina template. In these electrodes, the oxidation of glucose was enhanced with the increase in roughness factor. Furthermore, decrease in the influence of interferents such as L-ascorbic acid, uric acid, and p-acetamidophenol has been reported. Also, the electrode showed stable responses in the presence of chloride ions, which can be a cause of poisoning for noble metal electrodes.

Carbon nanotubes (CNTs) have also been used to improve the sensing performance. They are classified into single- and multi-walled tubes. The diameter of the former is typically 0.4–3 nm, whereas that of the latter ranges between 2 and 100 nm. The single-wall CNTs (SWCNTs) consist of a single cylindrical graphene sheet capped with hemispherical ends. The multi-wall CNTs (MWCNTs) consist of several to tens of concentric cylinders. Depending on the chirality of wrapping, CNTs show metallic or semiconducting properties.

Electrodes with a CNT/Nafion coating showed significant enhancement of sensitivity towards hydrogen peroxide and catecholamines [20]. Furthermore, the influence of interferents was suppressed significantly. Hrapovic et al. used SWCNTs and platinum nanoparticles immobilized with Nafion [21]. When compared with electrodes with only the CNTs or platinum nanoparticles, significantly larger current was observed. Also, due to the perm-selective nature of Nafion, no detectable responses were observed with L-ascorbic acid and uric acid of physiological concentrations.

An ensemble of MWCNTs also enhances direct oxidation of glucose in alkaline media [22]. The influence of poisoning by chloride ions was not observed. However, the influence of L-ascorbic acid and uric acid could not be eliminated completely. Enhancement of sensitivity is not limited to glucose. With single- or multi-wall CNTs, significant enhancement of sensitivity has also been reported for oxygen [23], dopamine [24, 25], epinephrine [25], L-ascorbic acid [25], and NADH [26].

The electrochemistry of CNTs is a little complicated, and it will not be appropriate to regard them as simple long electrodes of the nm order. Experimental facts accumulated up to now suggest that the open end of the MWCNT has a high electron transfer rate but the sidewall presents a low electron transfer rate [27, 28]. According to a recent report [29], however, the electrochemical activity

of the parts of CNTs depends on the species to be analyzed and the existence of oxygen-containing surface functionalities. The accumulation of evidence is still necessary to reach the final conclusion.

Other than the CNTs, graphene sheets are beginning to be used for electrochemical devices, and have a potential to realize performance better than that of the CNT-based devices [28]. However, because there are technical difficulties to handle them at present compared with CNTs, the graphene-based devices are not addressed here.

2.2 Promotion of Direct Electron Transfer

Nanostructures have an effect to promote direct electron transfer between biomolecules and an electrode. In many enzymes, redox centers are located in the core of proteins. Therefore, direct exchange of electrons is often difficult. To promote electron transfer, mediators or promoters have been used. However, enzymes with capability of direct electron exchange facilitate fabrication of biosensors. To this end, CNTs have been used because of the remarkable electrocatalytic properties. With CNTs, there is a possibility to place them close to the redox centers of the proteins. This is actually the case. In many of the reported cases, a layer of single-wall or multiwall CNTs is formed on a base electrode by casting a CNT solution and the redox proteins are just placed on it. CNT electrodes have shown superior performance in promoting direct electron transfer with glucose oxidase [30], cytochrome *c* [31, 32], horseradish peroxidase [33, 34], hemoglobin [35], myoglobin [34], and microperoxidase [36], which was not observed with only the base electrode.

As for the realization of direct electron transfer, various nanomaterials other than CNTs have been tried, and numerous papers have been published. When improving sensing performance using this approach, previous trials should be checked by focusing on specific cases.

2.3 Activation of Electrochemiluminescence

Electrochemiluminescence (ECL) is generated by converting electrochemical energy into radiative energy [37, 38]. Advantages of the ECL detection when compared with fluorometry are excellent sensitivity and selectivity, broad dynamic range, spatial controllability, low cost, and compatibility with separation techniques. In particular, the most unique feature of ECL is that it can be initiated and controlled by applying a potential to an electrode. Several different mechanisms of ECL have been proposed: (1) annihilation ECL, (2) co-reactant ECL, and (3) cathodic luminescence. Among them, most of the ECL systems have been developed based on the co-reactant ECL. The co-reactant refers to a species to produce reactive intermediates, which react with a luminophore to form excited

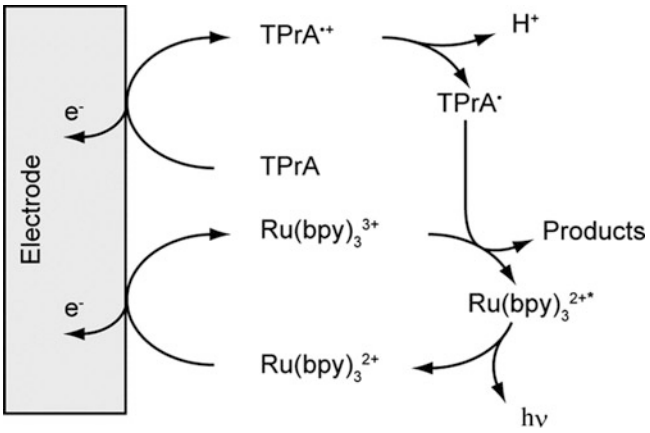

Fig. 7 Reaction mechanism of the $Ru(bpy)_3^{2+}$/TPrA ECL system

states of the luminophore. As an example, a widely used mechanism of tris(2,2′-bipyridyl)ruthenium (II) ($Ru(bpy)_3^{2+}$) and tri-*n*-propylamine (TPrA) system is described in Fig. 7.

Here, $Ru(bpy)_3^{2+}$ and TPrA are a luminophore and a co-reactant, respectively. First, $Ru(bpy)_3^{2+}$ is oxidized on the electrode. TPrA is also oxidized to produce a strong reductant TPrA•. Then, TPrA• and $Ru(bpy)_3^{3+}$ react to generate an excited state ($Ru(bpy)_3^{2+*}$) capable of emitting light. When the excited state returns to the ground state, luminescence whose emission peak is at 620 nm is emitted. Luminophores return to their initial state and can be used repeatedly, which is a marked contrast to luminophores used for chemiluminescence. This multiple excitation cycle amplifies the signal. On the other hand, the background signal is minimal because the stimulation mechanism is decoupled from light. The emitted light is detected using a commercial photomultiplier tube. The intensity of ECL depends on the applied potential and on the concentration of $Ru(bpy)_3^{2+}$ and TPrA.

To analyze nucleic acids, hybridization with DNA probes modified with ECL luminophores has been used. Zhang et al. reported a unique approach to detect a target single-strand DNA using a thiolated hairpin DNA tagged with $Ru(bpy)_3^{2+}$ assembled on a gold electrode (Fig. 8a) [39]. The hairpin DNA and the target DNA hybridize and form a rigid linear double-strand DNA (dsDNA), separating $Ru(bpy)_3^{2+}$ from the electrode. This results in the decrease of the ECL intensity, which can be used for DNA sensing. The lower detection limit was 90 pM. Intercalation of luminophore to dsDNA has also been used to enhance ECL. $[Ru(bpy)_2dppz]^{2+}$ (bpy = 2,2′-bipyridine; dppz = dipyrido[3,2-a:2′,3′-c]phenazine) itself emits negligible ECL. However, when it is intercalated into DNA, the ECL intensity increases by a factor of ~1,000 [40]. With a DNA aptamer against ATP, the ECL intensity decreases upon binding of ATP. With this technique, the lower

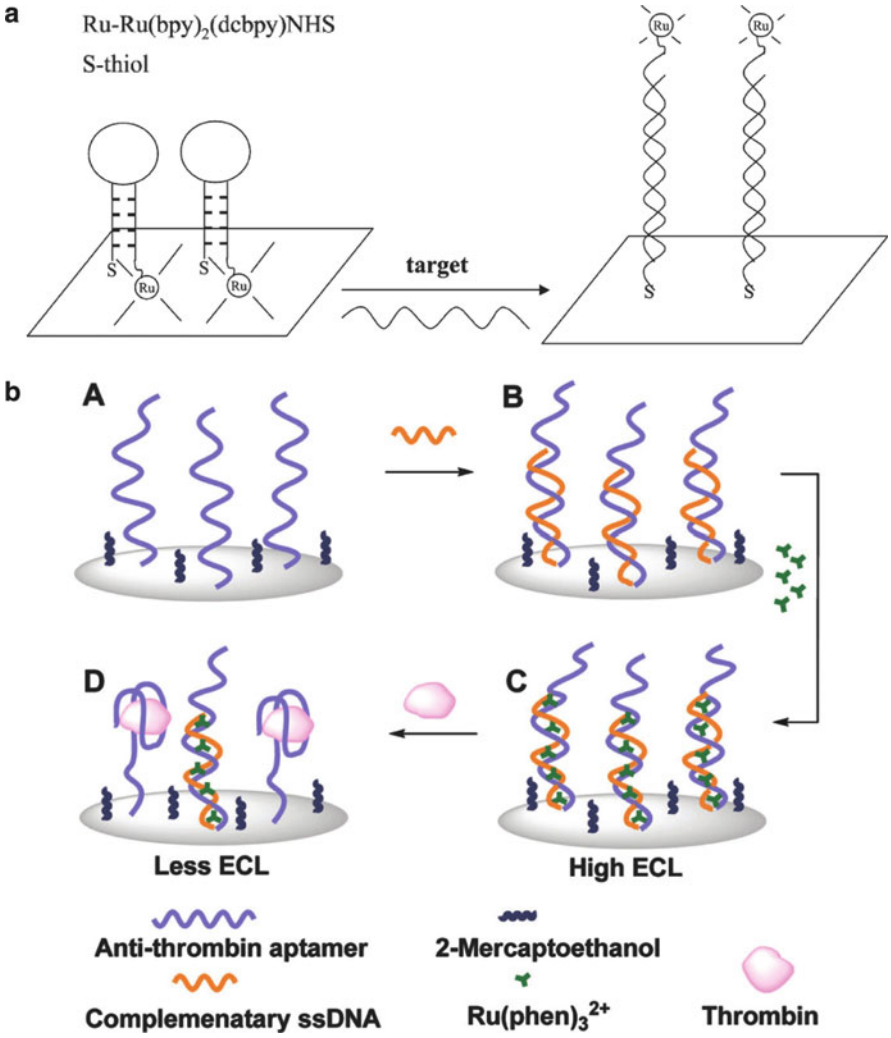

Fig. 8 ECL-based immunoassay. (**a**) Detection of DNA hybridization using hairpin-DNA probes. Reprinted with permission of [39]. Copyright 2008 American Chemical Society. (**b**) Detection of thrombin using label-free ECL aptasensors. (**A**) Attachment of the anti-thrombin thiolated aptamer to an electrode. (**B**) Formation of dsDNA with its cDNA. (**C**) Intercalation of $Ru(phen)_3^{2+}$ into the dsDNA. (**D**) Dissociation of dsDNA and release of $Ru(phen)_3^{2+}$ accompanying the binding of thrombin to its aptmer, resulting in the decrease of ECL. Reprinted with permission of [41]. Copyright 2009 American Chemical Society

detection limit was 100 nM [40]. The idea of using a DNA intercalator as an ECL fluorophore was further developed by Yin et al. (Fig. 8b) [41]. Their label-free ECL aptasensor was constructed based on the intercalation of $Ru(phen)_3^{2+}$ (phen = 1,10-phenanthroline) into dsDNA formed with an aptamer and its complementary DNA.

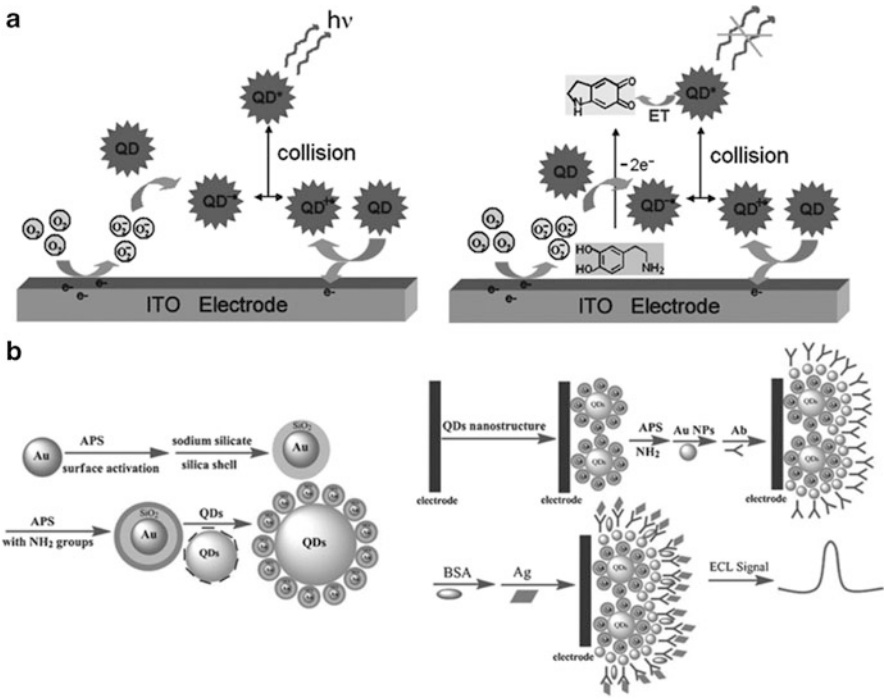

Fig. 9 Quantum-dot-based ECL. (**a**) ECL from QDs (*left*) and quenching (*right*). Reprinted with permission of [42]. Copyright 2007 American Chemical Society. (**b**) Synthesis of gold/silica/CdSe-CdS nanostructures (*left*) and fabrication of the ECL immunosensor (*right*). [44] – Reproduced by permission of The Royal Society of Chemistry

After the target molecule hybridized with its aptamer, the dsDNA dissociated and the intercalated $Ru(phen)_3^{2+}$ was released. The decrease in the ECL signal before and after the target molecule binding was used to quantify the concentration of the target molecule. For thrombin, the lower detection limit of 20 fM has been reported.

Unlike the other ECL methods, most of the quantum dots (QDs) ECL biosensors are developed based on quenching, inhibition, or enhancement of ECL. Quenching is caused by energy transfer between the excited QD and the analyte (or by-products generated from the analyte) when they are in close proximity. Liu et al. demonstrated an ECL quenching process of CdTe QDs and a new method to quantify catechol derivatives, which are ECL quenchers, as analytes (Fig. 9a) [42]. In the method, QD was excited by superoxide anion electrochemically generated at an electrode surface. In the presence of catechol derivatives, such as dopamine or L-adrenalin, energy transfer from the excited QDs to the catechol derivatives occurs, resulting in a significant decrease of ECL emission. The lower detection limit of dopamine was 50 nM.

One of the advantages of QDs is the easiness of functionalization. Yuan et al. reported signal amplification for ECL immunoassay [43]. In their system, cdse-cds nanoparticles were used as cores, which were covalently bound with QDs via polymer chains. The nanoparticles were further modified with antibodies to specifically bind target molecules. With the probe, the ECL measurement achieved 10 times as high sensitivity as that using unmodified QDs. The lower detection limit was a few pg mL^{-1}. As the other superstructure, a gold/silica/CdSe-CdS QD superstructure, formed by coating CdSe-CdS QDs with gold nanoparticles coated with SiO_2, emits ECL that is 17-fold higher than that from pure CdSe-CdS QDs (Fig. 9b) [44]. The structure was used for the detection of carcinoembryonic antigen, and a lower detection limit of 64 fg mL^{-1} has been achieved.

Detection sensitivity of ECL is significantly improved by using a SWCNT forest electrode. In the detection of a cancer marker, prostate specific antigen, that used nanoparticle labels containing $Ru(bpy)_3^{2+}$, 34-fold better sensitivity and 10-fold lower detection limit have been achieved compared with cases that used a pyrolytic graphite electrode [45]. CNT is also effective to enhance ECL from QDs. In the detection of H_2O_2, significant enhancement of ECL has been observed by using a CdS/CNT composite compared with the case without CNT [46].

In the detection of ECL using $Ru(bpy)_3^{2+}$, it is anticipated that the sensitivity is enhanced if $Ru(bpy)_3^{2+}$ ions are concentrated in the vicinity of an electrode. To this end, an effective approach is to use an ion-exchange polymer such as Nafion. With only this structure, the increase in the intensity of ECL was actually observed. However, by incorporating CNT further into this membrane, a 60-fold increase in the ECL intensity has been observed [47], which has been explained by an open structure realized accompanying the incorporation of CNT. Otherwise, co-reactants of $Ru(bpy)_3^{2+}$ can be concentrated on an electrode. In the enzymatic reaction of acetylcholinesterase, thiocholine is produced from acetylcholine. Thiocholine forms a monolayer on a gold electrode by gold-thiol bonding, which works as a concentrated layer of co-reactants for $Ru(bpy)_3^{2+}$ [48]. With antibodies labeled with the enzyme, anti tumor necrosis factor-α (TNF-α) of the sub-pM order has been detected by ELISA [48].

3 Fabrication of Nanoelectrode Arrays and Ensembles

The nanoelectrode structures discussed in previous sections are often similar. Therefore, it will be beneficial to describe the fabrication in a separate section to understand how these structures are formed. In this section, representative techniques to form nanoelectrode arrays and ensembles will be described. These techniques could be used independently or combined with other techniques to improve the detection performance.

3.1 Formation of Nanoelectrode Arrays by Electron-Beam Lithography or Focused Ion Beam Milling

IDAs can be formed by electron beam lithography [49]. By reducing the dimensions of the electrodes to the nm order, improvement of performance is expected. To realize it, techniques that are different from those used for microscale devices are used.

For the fabrication of electrodes of the μm order, photolithography is an appropriate choice. However, fabrication of electrodes with smaller dimensions must rely on other techniques. For electrodes of the sub-μm scale, electron-beam lithography has been used. Interdigitated electrodes of the sub-μm order have also been fabricated by deep UV lithography [50].

As a simple method, an array of nanoelectrodes can be formed by forming a layer of resist on a metal layer and by forming an array of nanoholes by the electron-beam lithography [51, 52]. Focused ion beam can also be used to form a nanoband electrode array. A platinum electrode pattern is formed by conventional photolithography and is passivated with a silicon nitride layer. Nano-scale openings are formed by milling the silicon nitride insulating layer to the bottom so that the underlying platinum is exposed (Fig. 10a) [53]. The exposed platinum areas work as the nanoelectrode array. Nanopore array electrodes have also been fabricated by this technique (Fig. 10b, c) [55].

By using additional techniques, the electrode size can be reduced further. Anisotropic etching is a technique often used for silicon bulk micromachining. This technique uses the difference in etching rates for various crystallographic orientations. The resulting structure can be used to shrink the patterns formed by electron-beam lithography (Fig. 11) [54]. After square patterns are formed in a silicon dioxide protecting layer formed on a very thin (100)-oriented silicon layer, the exposed areas of the silicon layer are anisotropically etched (Fig. 11a, b). This results in inverted pyramid through-holes (Fig. 11c, d). The dimensions of the through-holes formed on the other side of the silicon layer are much smaller than those formed in the silicon dioxide layer formed by electron-beam lithography. Nanoelectrodes with lateral dimensions of 15 nm have been obtained (Fig. 11e, f).

Conical microelectrodes have been fabricated by anisotropic etching of silicon (Fig. 10d) [56]. After the structure was formed, layers of insulators and platinum were formed. The platinum layer was exposed only at the tips by removing the outermost insulating layer after applying a photoresist.

Problems in the above-mentioned techniques are that they are high cost and low throughput. To solve this problem partially, a novel technique called nanoimprint lithography has been proposed (Fig. 10e) [57, 58]. In this method, a mold with nanostructures is first formed using the electron-beam lithography. This mold is then pressed into a thin film of thermoplastic polymer such as poly(methyl methacrylate) (PMMA) formed on a substrate that has been heated above its glass transition temperature. After separating the mold, the polymer residues in the compressed areas are removed by reactive ion etching. The patterns have been used to form interdigitated electrodes by a lift-off process [59, 60] or a nanodisc

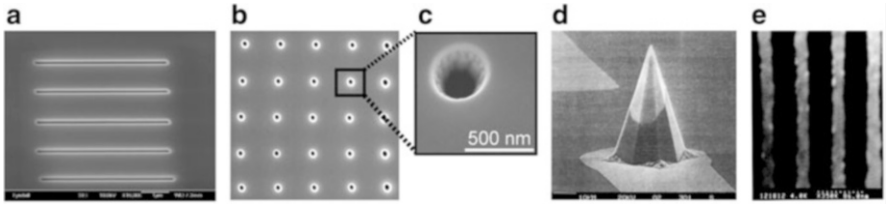

Fig. 10 SEM images of nanoelectrodes. (**a**) Nanoband electrode array fabricated by focused ion beam milling. Reprinted from [53], Copyright 2007, with permission from Elsevier. (**b**) Nanopore electrode array. (**c**) Magnified image of a nanopore. Adapted with permission from [55]. Copyright 2007 American Chemical Society. (**d**) Conical microelectrode with the platinum area exposed only at the tips. Reprinted from [56], Copyright 2000, with permission from Elsevier. (**e**) Metal lines (30 nm width and 70 nm pitch) fabricated by imprint lithography. Reprinted with permission from [58]. Copyright 1996, American Vacuum Society

electrode array by forming an insulating layer with an array of holes on a gold layer [52].

3.2 Formation of Nanoelectrode Arrays by Photolithography

In forming planar nanoelectrode arrays of controlled patterns, the electron-beam lithography is most widely used. Then, can't we form such nanoelectrode arrays if we do not have the very expensive instrument? The answer is yes. Some unique methods have been proposed based on patterning by ordinary photolithography.

An example is illustrated in Fig. 12 [61]. First, a nickel layer is deposited on a substrate, and photoresist patterns are formed. Then, the nickel layer is removed by electrochemically dissolving it. A point here is to overetch the nickel layer and form a horizontal trench under the photoresist layer. By depositing a metal such as gold, platinum, and palladium, and removing the photoresist and the nickel layer, nanoelectrode arrays can be obtained. The patterns of the nanoelectrodes can be designed in a desired manner and a long nanowire of the cm order can easily be obtained.

As already shown in Fig. 3, nanoelectrodes can also be formed on the cross-section of a sandwich structure. Single-band electrodes have been fabricated by depositing a metal electrode layer and an insulating layer and by exposing the electrode on one side [62–65]. Platinum and gold electrodes with widths of the nm order have been reported. Contrary to the width, the other dimension can be very long with this method. The cross section can be straight, circular, or a comb-like structure. The number of nanoelectrodes can be increased by stacking metal and insulator layers alternately [66].

In relation to this technique, a technique named "nanoskiving" has been proposed [67]. As in the previous cases, thin-film metal structures are embedded in epoxy. The epoxy matrix is then sectioned using an ultramicrotome. A section is placed on a substrate and epoxy is removed by oxygen plasma etching. Nanowires fabricated by this technique have been used for electroanalysis [68].

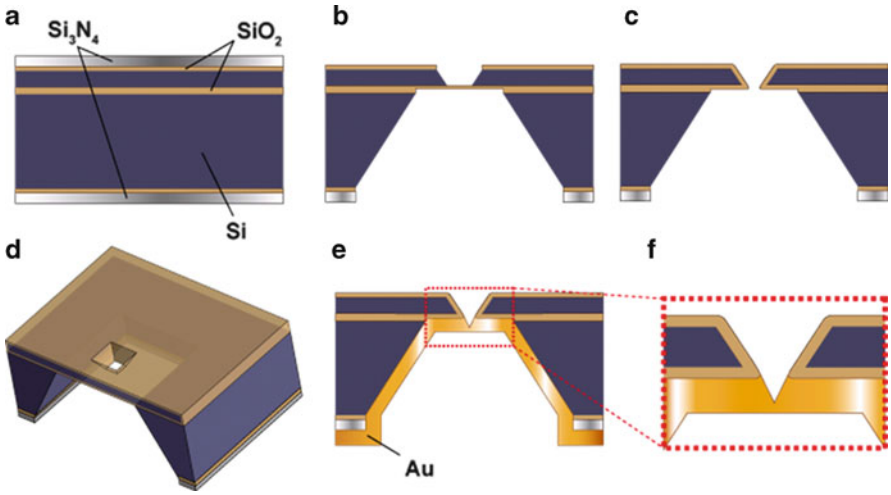

Fig. 11 Cross-sectional and three-dimensional illustrations of the fabrication process of a nanoelectrode using electron-beam lithography. (**a**) Si substrate covered with a SiO_2 layer and a Si_3N_4 layer. (**b**) Formation of a square pattern in the SiO_2 layer and anisotropic etching of the exposed Si layer. (**c**) Formation of pyramid-shaped holes through the wafer. (**d**) Three-dimensional view of the structure shown in (**c**). (**e**) Deposition of gold on one side of the device. (**e**) Magnified view of the nanoelectrode. Adapted with permission from [54]. Copyright 2005 American Chemical Society

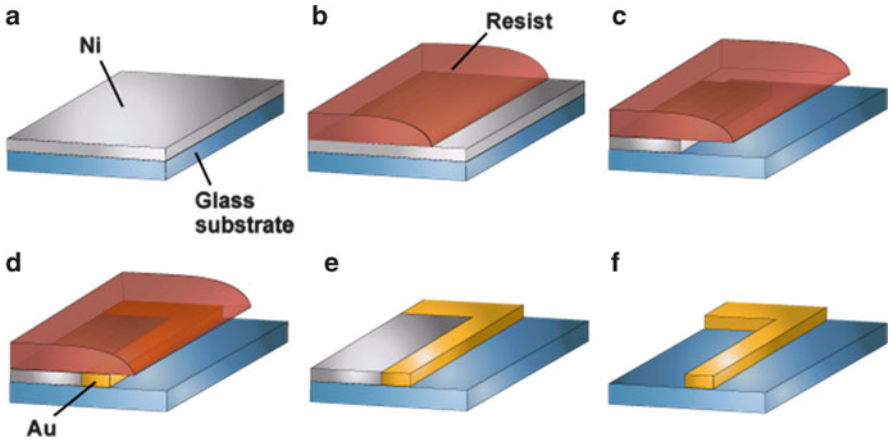

Fig. 12 Fabrication of a gold nanowire. (**a**) Deposition of a sacrificial Ni layer onto a glass substrate. (**b**) Formation of a photoresist pattern. (**c**) Overetching of the Ni layer. (**d**) Deposition of a gold layer into the trench between the photoresist and the glass substrate. (**e**) Photoresist removed. (**f**) Ni removed. Adapted by permission from Macmillan Publishers Ltd: [61], copyright 2006

3.3 Formation of a Layer of Randomly Oriented CNTs

CNTs activate electrode reactions. In taking advantage of this, the simplest method is to form a layer of randomly oriented CNTs by casting a solution containing CNTs. Here, a problem is unavailability of appropriate solvents [69]. CNTs can be made water-soluble by adsorbing surfactant molecules on the surface of CNTs [69–71]. CNTs are first dispersed in a solution of a surfactant whose concentration is higher than the critical micellar concentration, which is the concentration at which surfaces are saturated with surfactant and the surfactant molecules start self-aggregating into micelles. Then, the solution is sonicated. The solution is used to cast CNTs onto an appropriate substrate and form the layer. A concern with this method may be the existence of the surfactant, which may influence the physical properties of CNTs and induce unwanted chemical reactions. However, when the CNT layer is used for sensing, the surfactant can be removed by washing the layer with distilled water [69].

Solubility of CNT has also been improved by wrapping CNT in polymeric chains. Molecules of high molecular weight thread themselves onto or wrap themselves around the surfaces of CNTs and disrupt van der Waals interactions that cause CNTs to aggregate into bundles. For this purpose, poly (metaphenylne-vinylene) [72] or Nafion [20] has been used.

Solubilization of CNTs is a critical theme in many research fields. Therefore, many other methods have been developed and the effort continues even now [73].

3.4 Formation of CNT Nanoelectrode Ensembles

If CNTs are formed in a more controlled manner, nanoelectrode ensembles with appropriate interelectrode spacing could be realized by directly growing CNTs on a substrate. Low-density nanoelectrode arrays of CNTs have been fabricated by depositing Ni seeding nanoparticles first by electrochemical deposition and growing CNTs by plasma-enhanced chemical vapor deposition (Fig. 13) [74]. The CNTs were embedded in an epoxy layer. After polishing the surface, an array of tips of the CNT was obtained. Ni or NiFe alloy seeding spots can also be patterned by electron-beam lithography. Vertically aligned fibers with controlled interelectrode spacing have been fabricated [75–77].

3.5 Formation of Nanoelectrode Ensembles Using a Template

The porous structure of aluminum anodic oxide films has been used as a template to form various nanostructures [78]. Gold nanoelectrode ensembles were fabricated using this technique [79]. In forming the ensembles, a microporous oxide layer was first grown on an aluminum substrate. After the oxide layer was removed from the

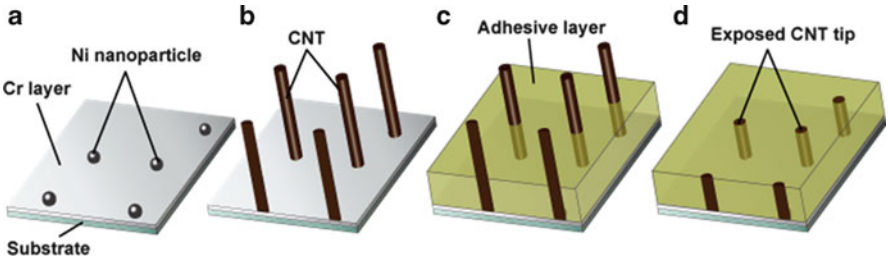

Fig. 13 Fabrication of a nanoelectrode array using vertically grown low-density CNTs. (**a**) Electrochemical deposition of Ni nanoparticles. (**b**) Growth of CNTs by plasma-enhanced chemical vapor deposition on the Ni particles. (**c**) Coating the surface with an adhesive. (**d**) Polishing of the adhesive layer. Adapted with permission from [74]. Copyright 2003 American Chemical Society

substrate to use it as a template, a gold layer was formed by vacuum-depositing gold onto the open ends of the pores. The side of the substrate covered with gold was attached to a glassy carbon electrode, and the other side of the porous oxide film was etched. As a result, the gold nanoelectrode ensemble was exposed.

Porous polycarbonate membranes have also been used as templates to form disk electrode ensembles of platinum [80] and gold [81]. The membranes were formed by an irradiation/chemical etch technique. In forming the ensemble of platinum electrodes, the membrane was fixed on a platinum electrode and platinum was deposited in the pores. After the pores were stuffed with platinum and the membrane surface was covered with overgrown platinum, the membrane surface was exposed again by removing the excess platinum [80]. The gold disk electrode ensembles were fabricated by depositing gold on the walls of nanopores by electroless deposition and following the same procedure [81]. With this technique, three-dimensional nanoelectrode ensembles can also be formed by partially or totally removing carbonate by dissolving it in an appropriate solvent such as dichloromethane [81] or by oxygen plasma etching [82].

3.6 Other Techniques

Nanoelectrode ensembles can be formed by opening up nanoholes in an insulating layer formed on an electrode. Defects in a self-assembled monolayer formed on a gold electrode work as nanoelectrode ensembles [83–85].

Like many other techniques to fabricate nanoelectrode ensembles, a problem is the control of pore size and distribution over the electrode surface. To solve this problem, the insulating film was formed with a highly ordered self-assembling block copolymer film [86]. The film is formed by spin-coating a polystylene (PS)/PMMA diblock copolymer solution onto a gold electrode. The dried film is then annealed in the presence of a strong electric field to orient the PMMA perpendicularly to the electrode surface. Exposure to UV radiation simultaneously cross-links

the PS and degrades the PMMA. The PMMA is finally dissolved in glacial acetic acid to form the pores.

Nanoelectrode ensembles can also be formed on a planar electrode even without an insulating layer. The overpotential to oxidize or reduce an electroactive analyte depends on the electrode material. Therefore, if nanoscale deposits of a metal that are active to an analyte are formed on a planar electrode of a different metal that is inactive to the analyte, the deposits work as a nanoelectrode ensemble. Platinum black particles were deposited on a gold electrode to form a nanoelectrode ensemble of platinum black. A significant enhancement of sensitivity to H_2O_2 was observed compared with the planar gold electrode used as the base electrode [15].

4 Concluding Remarks

In this chapter, techniques to improve the detection sensitivity of electrochemical microdevices were reviewed. Here, a convincing conclusion is that nanotechnology really has an effect for this purpose. Reflecting the fact and growing expectations, various nanomaterials such as nanotubes, nanowires, and nanoparticles have been used very actively. As a result, numerous papers have been published and the tendency continues even now [87–90]. At present, the application of nanotechnology to electrochemical microdevices is limited. However, with the wealth of knowledge of nanotechnology, devices whose performance is comparable with or better than those of macroscopic counterparts used for ordinary electroanalysis will surely be realized.

References

1. Wightman RM (1981) Microvoltammetric electrodes. Anal Chem 53(9):1125A–1134A
2. Niwa O (1995) Electroanalysis with interdigitated array microelectrodes. Electroanalysis 7(7):606–613
3. Štulík K, Amatore C, Holub K, Mareček V, Kutner W (2000) Microelectrodes. Definitions, characterization, and applications. Pure Appl Chem 72(8):1483–1492
4. Aoki A, Matsue T, Uchida I (1990) Electrochemical response at microarray electrodes in flowing streams and determination of catecholamines. Anal Chem 62:2206–2210
5. Vandaveer IV WR, Woodward DJ, Fritsch I (2003) Redox cycling measurements of a model compound and dopamine in ultrasmall volumes with a self-contained microcavity device. Electrochim Acta 48:3341–3348
6. Zevenbergen MAG, Krapf D, Zuiddam MR, Lemay SG (2007) Mesoscopic concentration fluctuations in a fluidic nanocavity detected by redox cycling. Nano Lett 7(2):384–388
7. Wolfrum B, Zevenbergen M, Lemay S (2008) Nanofluidic redox cycling amplification for the selective detection of catechol. Anal Chem 80:972–977
8. Zevenbergen MAG, Wolfrum BL, Goluch ED, Singh PS, Lemay SG (2009) Fast electron-transfer kinetics probed in nanofluidic channels. J Am Chem Soc 131:11471–11477

9. Kätelhön E, Hofmann B, Lemay SG, Zevenbergen MAG, Offenhäusser A, Wolfrum B (2010) Nanocavity redox cycling sensors for the detection of dopamine fluctuations in microfluidic gradients. Anal Chem 82:8502–8509
10. Łoś M, Łoś JM, Blohm L, Spillner E, Grunwald T, Albers J, Hintsche R, Węgrzyn G (2005) Rapid detection of viruses using electrical biochips and anti-virion sera. Lett Appl Microbiol 40:479–485
11. Bange A, Tu J, Zhu X, Ahn C, Halsall HB, Heineman WR (2007) Electrochemical detection of MS2 phage using a bead-based immunoassay and a nanoIDA. Electroanalysis 19 (21):2202–2207
12. Nebling E, Grunwald T, Albers J, Schäfer P, Hintsche R (2004) Electrical detection of viral DNA using ultramicroelectrode arrays. Anal Chem 76:689–696
13. Elsholz B, Wörl R, Blohm L, Albers J, Feucht H, Grunwald T, Jürgen B, Schweder T, Hintsche R (2006) Automated detection and quantitation of bacterial RNA by using electrical microarrays. Anal Chem 78:4794–4802
14. Albers J, Grunwald T, Nebling E, Piechotta G, Hintsche R (2003) Electrical biochip technology – a tool for microarrays and continuous monitoring. Anal Bioanal Chem 377:521–527
15. Niwa O, Horiuchi T, Morita M, Huang T, Kissinger PT (1996) Determination of acetylcholine and choline with platinum-black ultramicroarray electrodes using liquid chromatography with a post-column enzyme reactor. Anal Chim Acta 318:167–173
16. Evans SAG, Elliott JM, Andrews LM, Bartlett PN, Doyle PJ, Denuault G (2002) Detection of hydrogen peroxide at mesoporous platinum microelectrodes. Anal Chem 74:1322–1326
17. Song Y-Y, Zhang D, Gao W, Xia X-H (2005) Nonenzymatic glucose detection by using a three-dimensionally ordered, macroporous platinum template. Chem Eur J 11:2177–2182
18. Park S, Chung TD, Kim HC (2003) Nonenzymatic glucose detection using mesoporous platinum. Anal Chem 75:3046–3049
19. Yuan J, Wang K, Xia X (2005) Highly ordered platinum-nanotubule arrays for amperometric glucose sensing. Adv Funct Mater 15(5):803–809
20. Wang J, Musameh M, Lin Y (2003) Solubilization of carbon nanotubes by nafion toward the preparation of amperometric biosensors. J Am Chem Soc 125:2408–2409
21. Hrapovic S, Liu Y, Male KB, Luong JHT (2004) Electrochemical biosensing platforms using platinum nanoparticles and carbon nanotubes. Anal Chem 76:1083–1088
22. Ye J-S, Wen Y, Zhang WD, Gan LM, Xu GQ, Sheu F-S (2004) Nonenzymatic glucose detection using multi-walled carbon nanotube electrodes. Electrochem Commun 6:66–70
23. Britto PJ, Santhanam KSV, Rubio A, Alonso JA, Ajayan PM (1999) Improved charge transfer at carbon nanotube electrodes. Adv Mater 11(2):154–157
24. Britto PJ, Santhanam KSV, Ajayan PM (1996) Carbon nanotube electrode for oxidation of dopamine. Bioelectrochem Bioenerg 41:121–125
25. Luo H, Shi Z, Li N, Gu Z, Zhuang Q (2001) Investigation of the electrochemical and electrocatalytic behavior of single-wall carbon nanotube film on a glassy carbon electrode. Anal Chem 73:915–920
26. Musameh M, Wang J, Merkoci A, Lin Y (2002) Low-potential stable NADH detection at carbon-nanotube-modified glassy carbon electrodes. Electrochem Commun 4:743–746
27. Dumitrescu I, Unwin PR, Macpherson JV (2009) Electrochemistry at carbon nanotubes: perspective and issues. Chem Commun 6886–6901
28. Yang W, Ratinac KR, Ringer SP, Thordarson P, Gooding JJ, Braet F (2010) Carbon nanomaterials in biosensors: should you use nanotubes or graphene? Angew Chem Int Ed 49:2114–2138
29. Gong K, Chakrabarti S, Dai L (2008) Electrochemistry at carbon nanotube electrodes: is the nanotube tip more active than the sidewall? Angew Chem Int Ed 47:5446–5450
30. Cai C, Chen J (2004) Direct electron transfer of glucose oxidase promoted by carbon nanotubes. Anal Biochem 332:75–83
31. Wang G, Xu J-J, Chen H-Y (2002) Interfacing cytochrome *c* to electrodes with a DNA - carbon nanotube composite film. Electrochem Commun 4:506–509

32. Wang J, Li M, Shi Z, Li N, Gu Z (2002) Direct electrochemistry of cytochorome *c* at a glassy carbon electrode modified with single-wall carbon nanotubes. Anal Chem 74:1993–1997
33. Zhao Y-D, Zhang W-D, Chen H, Luo Q-M, Li SFY (2002) Direct electrochemistry of horseradish peroxidase at carbon nanotube powder microelectrode. Sens Actuators B 87:168–172
34. Yu X, Chattopadhyay D, Galeska I, Papadimitrakopoulos F, Rusling JF (2003) Peroxidase activity of enzymes bound to the ends of single-wall carbon nanotube forest electrodes. Electrochem Commun 5:408–411
35. Cai C, Chen J (2004) Direct electron transfer and bioelectrocatalysis of hemoglobin at a carbon nanotube electrode. Anal Biochem 325:285–292
36. Gooding JJ, Wibowo R, Liu J, Yang W, Losic D, Orbons S, Mearns FJ, Shapter JG, Hibbert DB (2003) Protein electrochemistry using aligned carbon nanotube arrays. J Am Chem Soc 125:9006–9007
37. Richter MM (2004) Electrochemiluminescence (ECL). Chem Rev 104:3003–3036
38. Miao W (2008) Electrogenerated chemiluminescence and its biorelated applications. Chem Rev 108:2506–2553
39. Zhang J, Qi H, Li Y, Yang J, Gao Q, Zhang C (2008) Electrogenerated chemiluminescence DNA biosensor based on hairpin DNA probe labeled with ruthenium complex. Anal Chem 80:2888–2894
40. Hu L, Bian Z, Li H, Han S, Yuan Y, Gao L, Xu G (2009) $[Ru(bpy)_2dppz]^{2+}$ electrochemiluminescence switch and its applications for DNA interaction study and label-free ATP aptasensor. Anal Chem 81:9807–9811
41. Yin X-B, Xin Y-Y, Zhao Y (2009) Label-free electrochemiluminescent aptasensor with attomolar mass detection limits based on a $Ru(phen)_3^{2+}$-double-strand DNA composite film electrode. Anal Chem 81:9299–9305
42. Liu X, Jiang H, Lei J, Ju H (2007) Anodic electrochemiluminescence of CdTe quantum dots and its energy transfer for detection of catechol derivatives. Anal Chem 79(21):8055–8060
43. Yuan L, Hua X, Wu Y, Pan X, Liu S (2011) Polymer-functionalized cdse-cds nanosphere labels for ultrasensitive detection of tumor necrosis factor-alpha. Anal Chem 83:6800–6809
44. Jie G-F, Liu P, Zhang S-S (2010) Highly enhanced electrochemiluminescence of novel gold/silica/CdSe-CdS nanostructures for ultrasensitive immunoassay of protein tumor marker. Chem Commun 46:1323–1325
45. Sardesai N, Pan S, Rusling J (2009) Electrochemiluminescent immunosensor for detection of protein cancer biomarkers using carbon nanotube forests and $[Ru\text{-}(bpy)_3]^{2+}$-doped silica nanoparticles. Chem Commun 4968–4970
46. Ding S-N, Xu J-J, Chen H-Y (2006) Enhanced solid-state electrochemiluminescence of CdS nanocrystals composited with carbon nanotubes in H_2O_2 solution. Chem Commun 3631–3633
47. Guo Z, Dong S (2004) Electrogenerated chemiluminescence from $Ru(bpy)_3^{2+}$ ion-exchanged in carbon nanotube/perfluorosulfonated ionomer composite films. Anal Chem 76:2683–2688
48. Kurita R, Arai K, Nakamoto K, Kato D, Niwa O (2010) Development of electrogenerated chemiluminescence-based enzyme linked immunosorbent assay for sub-pM detection. Anal Chem 82:1692–1697
49. Ueno K, Hayashida M, Ye J-Y, Misawa H (2005) Fabrication and electrochemical characterization of interdigitated nanoelectrode arrays. Electrochem Commun 7:161–165
50. van Gerwen P, Laureyn W, Laureys W, Huyberechts G, de Beeck MO, Baert K, Suls J, Sansen W, Jacobs P, Hermans L, Mertens R (1998) Nanoscaled interdigitated electrode arrays for biochemical sensors. Sens Actuators B 49:73–80
51. Hepel T, Osteryoung J (1986) Electrochemical characterization of electrodes with submicrometer dimensions. J Electrochem Soc 133(4):752–757
52. Sandison ME, Cooper JM (2006) Nanofabrication of electrode arrays by electron-beam and nanoimprint lithographies. Lab Chip 6:1020–1025
53. Lanyon YH, Arrigan DWM (2007) Recessed nanoband electrodes fabricated by focused ion beam milling. Sens Actuators B 121:341–347

54. Lemay SG, van den Broek DM, Storm AJ, Krapf D, Smeets RMM, Heering HA, Dekker C (2005) Lithographycally fabricated nanopore-based electrodes for electrochemistry. Anal Chem 77:1911–1915
55. Lanyon YH, Marzi GD, Watson YE, Quinn AJ, Gleeson JP, Redmond G, Arrigan DWM (2007) Fabrication of nanopore array electrodes by focused ion beam milling. Anal Chem 79:3048–3055
56. Thiébaud P, Beuret C, de Rooij NF, Koudelka-Hep M (2000) Microfabrication of Pt-tip microelectrodes. Sens Actuators B 70:51–56
57. Chou SY, Krauss PR, Renstrom PJ (1996) Imprint lithography with 25-nanometer resolution. Science 272:85–87
58. Chou SY, Krauss PR, Renstrom PJ (1996) Nanoimprint lithography. J Vac Sci Technol B 14 (6):4129–4133
59. Montelius L, Heidari B, Graczyk M, Maximov I, Sarwe E-L, Ling TGI (2000) Nanoimprint- and UV-lithography: Mix&Match process for fabrication of interdigitated nanobiosensors. Microelectron Eng 53:521–524
60. Beck M, Persson F, Carlberg P, Graczyk M, Maximov I, Ling TGI, Montelius L (2004) Nanoelectrochemical transducers for (bio-) chemical sensor applications fabricated by nanoimprint lithography. Microelectron Eng 73–74:837–842
61. Menke EJ, Thompson MA, Xiang C, Yang LC, Penner RM (2006) Lithographically patterned nanowire electrodeposition. Nat Mater 5:914–919
62. Nagale MP, Fritsch I (1998) Individually addressable, submicrometer band electrode arrays. 1. Fabrication from multilayered materials. Anal Chem 70:2902–2907
63. Morris RB, Franta DJ, White HS (1987) Electrochemistry at Pt band electrodes of width approaching molecular dimensions. Breakdown of transport equations at very small electrodes. J Phys Chem 91:3559–3564
64. Samuelsson M, Armgarth M, Nylander C (1991) Microstep electrodes: band ultramicroelectrodes fabricated by photolithography and reactive ion etching. Anal Chem 63:931–936
65. Caston SL, McCarley RL (2002) Characteristics of nanoscopic Au band electrodes. J Electroanal Chem 529:124–134
66. Odell DM, Bowyer WJ (1990) Fabrication of band microelectrode arrays from metal foil and heat-sealing fluoropolymer film. Anal Chem 62:1619–1623
67. Xu Q, Rioux RM, Whitesides GM (2007) Fabrication of complex metallic nanostructures by nanoskiving. ACS Nano 1(3):215–227
68. Dawson K, Strutwolf J, Rodgers KP, Herzog G, Arrigan DWM, Quinn AJ, O'Riordan A (2011) Single nanoskived nanowidres for electrochemical applications. Anal Chem 83:5535–5540
69. Bonard J-M, Stora T, Salvetat J-P, Maier F, Stöckli T, Duschl C, Forró L, de Heer WA, Châtelain A (1997) Purification and size-selection of carbon nanotubes. Adv Mater 9 (10):827–831
70. O'Connel MJ, Bachilo SM, Huffman CG, Moore VC, Strano MS, Haroz EH, Rialon KL, Boul PJ, Noon WH, Kittrell C, Ma J, Hauge RH, Weisman RB, Smalley RE (2002) Band gap fluorescence from individual single-walled carbon nanotubes. Science 297:593–596
71. Richard C, Balavoine F, Schultz P, Ebbesen TW, Mioskowski C (2003) Supramolecular self-assembly of lipid derivatives on carbon nanotubes. Science 300:775–778
72. Star A, Stoddart JF, Steuerman D, Diehl M, Boukai A, Wong EW, Yang X, Chung S-W, Choi H, Heath JR (2001) Preparation and properties of polymer-wrapped single-walled carbon nanotubes. Angew Chem Int Ed 40(9):1721–1725
73. Merkoçi A, Pumera M, Llopis X, Pérez B, del Valle M, Alegret S (2005) New materials for electrochemical sensing VI: carbon nanotubes. Trends Anal Chem 24(9):826–838
74. Tu Y, Lin Y, Ren ZF (2003) Nanoelectrode arrays based on low site density aligned carbon nanotubes. Nano Lett 3(1):107–109

75. Ren ZF, Huang ZP, Wang DZ, Wen JG, Xu JW, Wang JH, Calvet LE, Chen J, Klemic JF, Reed MA (1999) Growth of a single freestanding multiwall carbon nanotube on each nanonickel dot. Appl Phys Lett 75(8):1086–1088
76. Guillorn MA, McKnight TE, Melechko A, Merkulov VI, Britt PF, Austin DW, Lowndes DH, Simpson ML (2002) Individually addressable vertically aligned carbon nanofiber-based electrochemical probes. J Appl Phys 91(6):3824–3828
77. Koehne J, Li J, Cassell AM, Chen H, Ye Q, Ng HT, Han J, Meyyappan M (2004) The fabrication and electrochemical characterization of carbon nanotube nanoelectrode arrays. J Mater Chem 14:676–684
78. Masuda H, Fukuda K (1995) Ordered metal nanohole arrays made by a two-step replication of honeycomb structures of anodic alumina. Science 268:1466–1468
79. Uosaki K, Okazaki K, Kita H, Takahashi H (1990) Preparative method for fabricating a microelectrode ensemble: electrochemical response of microporous alminum anodic oxide film modified gold electrode. Anal Chem 62:652–656
80. Penner RM, Martin CR (1987) Prepararion and electrochemical characterization of ultramicroelectrode ensembles. Anal Chem 59:2625–2630
81. Menon VP, Martin CR (1995) Fabrication and evaluation of nanoelectrode ensembles. Anal Chem 67:1920–1928
82. Yu S, Li N, Wharton J, Martin CR (2003) Nano wheat fields prepared by plasma-etching gold nanowire-containing membranes. Nano Lett 3(6):815–818
83. Sabatani E, Rubinstein I (1987) Organized self-assembling monolayers on electrodes. 2. Monolayer-based ultramicroelectrodes for the study of very rapid electrode kinetics. J Phys Chem 91:6663–6669
84. Chailapakul O, Sun L, Xu C, Crooks RM (1993) Interactions between organized, surface-confined monolayers and vapor-phase probe molecules. 7. Comparison of self-assembling *n*-alkanethiol monolayers deposited on gold from liquid and vapor phases. J Am Chem Soc 115:12459–12467
85. Che G, Cabrera CR (1996) Molecular recognition based on (3-mercaptopropyl) trimethoxysilane modified gold electrodes. J Electroanal Chem 417:155–161
86. Jeoung E, Galow TH, Schotter J, Bal M, Ursache A, Tuominen MT, Stafford CM, Russell TP, Rotello VM (2001) Fabrication and characterization of nanoelectrode arrays formed via block copolymer self-assembly. Langmuir 17:6396–6398
87. Arrigan DWM (2004) Nanoelectrodes, nanoelectrode arrays and their applications. Analyst 129:1157–1165
88. Pumera M, Sánchez S, Ichinose I, Tang J (2007) Electrochemical nanobiosensors. Sens Actuators B 123:1195–1205
89. Noy A (2011) Bionanoelectronics. Adv Mater 23:807–820
90. Rassaei L, Singh PS, Lemay SG (2011) Lithography-based nanoelectrochemistry. Anal Chem 83:3974–3980